JCHR (2024) 14(3), 537-553

Journal of Chemical Health Risks

sanad.iau.ir/journal/jchr

ORIGINAL ARTICLE

Assessment of Antibacterial, Antioxidant, and Catalytic Activity of Zinc Oxide Nanoparticles Biosynthesized by Pistacia Vera Soft Waste Peel Extract

Hossein Golchinpour, Alireza Momeni, Mohammad Hadi Meshkatalsadat*

Department of Chemistry, Qom University of Technology, Qom, Iran

(Received: 18 February 2023 Accepted: 11 April 2024)

KEYWORDS

Antibacterial;
Antioxidant;
Dye reduction;
Green synthesis;
Escherichia coli;
Staphylococcus aureus

ABSTRACT: The green synthesis of metal oxide nanoparticles using plant extracts can effectively replace traditional chemical synthesis methods. In present paper, we describe the formation of zinc oxide (ZnO) nanoparticles (NPs) using *Pistacia vera* soft peel extract. Synthesis of plant-based nanoparticles possesses numerous advantages compared to the conventional physicochemical approaches with different applications in biology and medicine. In the present study *Pistacia vera* peel extract was used to synthesize ZnO NPs. To investigate the optical and structural features of ZnO nanoparticles synthesized by *Pistacia vera* peel extract, X-ray diffraction (XRD), Fourier transform infrared (FTIR) spectroscopy, ultraviolet-visible spectrophotometer (UV-Vis), and scanning electron microscope (SEM) were used. The off-yellow hue of the reaction mixture indicated that ZnO NPs were formed. The presence of *Pistacia vera* peel extract-mediated ZnO NPs was revealed by UV-Visible peaks at 422 nm. In addition, an XRD pattern confirmed the formation of spherical structure nanomaterials with an average size of 42 nm along with the XRD pattern matching the JCPDS card. The Existence of bioactive functional groups effective in reducing the bulk of zinc sulfate to ZnO NPs was further confirmed by FTIR. The SEM images revealed the spherical shape, and the size of nanoparticles, which was within the range of 31.14 to 48 nm. To examine the antibacterial potential of ZnO NPs, a paper disc diffusion technique was used against Gram-negative *Escherichia coli* and Gram-positive *Staphylococcus aureus* clinical strains in terms of the inhibition zone. In addition, the radical scavenging assay was done by the DPPH test. The green synthesized Pistacia peel extract-mediated ZnO NPs demonstrate striking antioxidative activity at 100 µg mL^{-1}. Using $NaBH_4$, nanoscale zinc oxide can remove methylene blue in only 150 seconds. Furthermore, they remove 98% of methylene blue in 14 minutes under UV light.

INTRODUCTION

In nanotechnology, novel nanometer-scale materials are created by using technology that is both emerging and innovative. Compared to materials with undefined particle sizes, nanomaterials have a striking surface area, quantum size, volume, and macro tunneling properties [1]. Nanoparticles possess significant optical-mechanical, biological, and catalytic properties. These properties provide extensive application potential for nanomaterials [2]. ZnO NPs are used in medical devices, electrochemistry, cosmetics, and textiles [3]. The synthesizing of ZnO NPs is generally done chemically or physically, with several drawbacks such as low purity, uneven particle size distribution, high energy usage, massive amounts of secondary waste, and environmental pollution [4, 5]. Researchers have been interested in metal oxide nanoparticles, including ZnO, due to their

*Corresponding author: meshkatalsadat.m@qut.ac.ir (M. H. Meshkatalsadat)
DOI: 10.60829/jchr.2024.1687

unique chemical and optical properties, which can easily be tuned by altering the morphology [6, 7]. ZnO NPs have been utilized in different innovative applications such as electronics, sensors, cosmetics, communication, environmental protection, medicinal industry, and biology [8-11]. As part of the branch of environmental applications, one of these applications entails the removal of organic dyes from aquatic environments that are harmful to the environment. By exposing these nanoparticles to a stimulating factor, such as $NaBH_4$, sunlight or UV radiation, these nanoparticles become activated and remove the polluting color. It is their photocatalytic property that allows these nanoparticles to be activated under light condition [5-8]. As of today, these nanoparticles have been tested against several polluting dyes, including congo red [6], malachite green [12], azo dyes [13], and methylene blue [14].

Enzymes, plant extracts, and microorganisms are incorporated into the green synthesis procedure, which leads to energy saving while toxic substances are no longer used in the process [15]. It has several advantages, including being environmentally friendly, inexpensive, and non-toxic. It therefore, represents an exciting alternative to traditional chemical and physical methods [16, 17]. The plants and their extracts are easily sourced, and the zinc salt solution is used only as a precursor to the metal during the process. As a result of the reaction between plant extracts and zinc salt solution, ZnO NPs are synthesized. These valuable nanomaterials have remarkable applications in biochemistry and biomedical such as antimicrobial and antioxidant properties, drug delivery, and sunscreen, while they are striking too in industry applications, including coating, cosmetics, photocatalysis, pesticides, agriculture, and organic dye reduction [16-20]. As a result of the superior antimicrobial properties of ZnO NPs, they have various applications in surgical tapes, calamine lotions, and shampoos. These nanoparticles display a broad spectrum of antibacterial effects at deficient concentrations [20]. There has been tremendous interest in using ZnO NPs for biological applications, such as biological sensing, biological labeling, gene and drug delivery, and nanomedicine [22].

The pistachio tree is native to central Asia, mainly Afghanistan and Iran. Pistachio, (*Pistacia vera*), a small tree of Anacardiaceae (the cashew family), and its edible seeds, are grown in drylands in temperate or warm climates. It is believed that the pistachio tree is indigenous to Iran. It is cultivated extensively from Afghanistan to the Mediterranean region. The seed kernels can be consumed roasted or fresh. They are used commonly in various desserts such as Baklava, Halvah, and ice cream, as well as for foods flavored pistachio with green coloring. The seeds are enriched in protein, vitamin B6, and dietary fiber [23].

As part of this study, we intend to perform a safe and environmentally friendly synthesis in accordance with all the principles of green chemistry. To achieve this goal, we use a plant waste precursor, the pistachio soft peel, as the principal source of synthesis. This study attempts to produce a multipurpose nanoparticle and explores its properties and applications using a variety of methods. Using UV-Vis spectroscopy, FT-IR, XRD, SEM, and EDX, the physicochemical properties of these nanoparticles will be investigated. Antibacterial and antioxidant properties of these nanoparticles are studied by disc diffusion and DPPH methods. In the third part of this study, we will examine one of the most remarkable applications in light of the second objective of this study, which is the synthesis of safe nanocatalysts capable of removing organic dyes from the aqueous environment at a faster rate than other nanocatalysts. In order to assess the dye degradation activity of these nanomaterials in the removal of methylene blue, we use NaBH4 as a reduction agent in the catalytic reaction and UV light as an activator in the photocatalytic reaction.

MATERIALS AND METHODS

Pistacia vera skin extract preparation

Pistacia vera (*p. vera*) fresh peel was aggregated from the Pistachio Garden around Qom city, the capital city of Qom Province, Iran. Separated pistachio peels thoroughly rinsed with tap water three times before washing with deionized water, then dried away from direct sunlight for three weeks under shade. Boiling the *P. vera* peel in the deionized water at 70°C for 45 minutes, the *P. vera* peel extract was filtered to eliminate the insoluble macromolecules and fractions. By using the obtained extract, the capping and reducing agent were

provided by phenols and polyphenols present in the extract.

Green synthesis of ZnO NPs

Mixing 90 ml of aqueous zinc sulfate ($ZnSO_4$.7 H_2O Merck® 108883) solution (1.5 mM) with 10 ml of the *P. vera* peel extract, treated with 10 ml 0.5 M sodium hydroxide (Merck® 106498) was performed to set the PH to 12 as optimum PH. The incubation of the reaction mixture was performed while stirring constantly at 60 °C in the dark. The zinc sulfate in deionized water presented the ions initiating the reaction. The formation of ZnO NPs was revealed by an off-yellow color after 1 h. By the first separation of the nanoparticles via centrifuging, the loosened material was eliminated for 15 min at 10000 rpm, which was washed three times in a row with ethanol and deionized water. Once centrifuging, the mixture was dehumidified at 90^{o}c by oven. Figure 1 provides a brief overview of this facile and economic approach of green synthesis of ZnO NPs by *P. vera* soft peel extract.

Characterization of ZnO NPs

Nanoparticle characteristics can be detected using methods such as microscopy and non-microscopy, including ultraviolet visible spectroscopy, Electron dispersive X-ray spectroscopy, Fourier transform infrared spectroscopy, Dynamic light scattering, and Electron microscopy. The dried ZnO NPs biosynthesized in this study have been analyzed using several techniques, including UV-visible, FTIR, SEM, and XRD.

UV-Vis characterization

Utilizing ultraviolet-visible spectrophotometry, ZnO NPs were characterized for their maximum absorbance. UV-Vis spectral analysis was performed using a Physicminiature UVS-2500 spectrophotometer. UV-visible absorption spectrophotometer was used with a resolution of 1 nm within 300-800 nm.

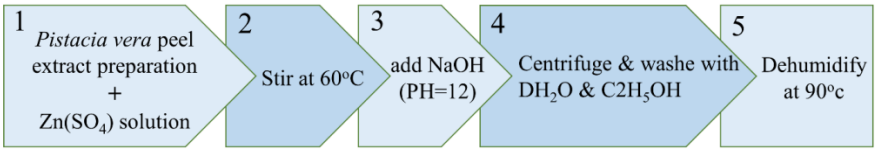

Figure 1. Short frame of facile synthesis of *P. vera*-mediated ZnO NPs

Fourier-transform infrared spectroscopy (FTIR)

The Thermo/Nicolet Avatar 360 FTIR Spectrometer system was used to record the functional group of the nanomaterials in the transmittance mode in the range of 400–4000 cm^{-1}. As infrared radiation bombards the synthesized ZnO nanoparticles sample, some radiations are attracted while others are not. Radiation emitted from unabsorbed ZnO NPs leaves a specific fingerprint that indicates their characteristics [24]. FTIR helps to determine the efficiency of plant extracts as reducing agents [25]. Advantageous functional groups in biomolecules in extracts including O-H, C=O, C=C, C-N, C-H, and N-H, appear in FTIR analysis, and they are significant reducing agents for ZnO NPs synthesis [26].

XRD

The crystal structure of ZnO NPs was determined utilizing XRD Philips PW1730. Throughout XRD analysis, ZnO NPs are brought into the energetic rays from the XRD device that penetrate it to provide valuable data on its structure. In the XRD pattern, the broadening represents the nano size. The Debye Scherer's equation ($d = k \lambda / \beta \cos \theta$) is used to estimate the average scale of the ZnO NPs [27, 28].

Scanning electron microscope (SEM)

The imaging of the surface of a sample at the nano and microscale is performed with an electron beam to obtain high-resolution images of the structure of the sample [29]. The surface topology of ZnO NPs can be assessed using SEM images by adjusting the density of the electron on the surface and increasing the magnification and field depth [30]. The detector generates and records signals by presenting electron beams to ZnO NPs. From recorded signals, the morphology, orientation, and crystalline structure of ZnO NPs are inferred [31]. ZnO NPs were examined under SEM (Tescan Mira3) in order

to study their surface morphology, size, and shape.

EDX

To gain a deeper understanding of the characteristics of phyto-synthesized ZnO NPs, an analysis of the sample was conducted using energy-dispersive X-ray spectroscopy (TESCAN MIRA II). In EDX analysis, an electron beam hits an atom's inner shell, knocking an electron off and leaving behind a positively charged electron-hole. Upon displacement of an electron, another electron from an outer shell fills the vacancy. By moving from the exterior, higher-energy shell of the atom to the inner, lower-energy surface, the electron releases the energy difference in the form of an X-ray. A characteristic energy is associated with each of the elements and transitions in X-rays. By identifying the peaks, the elements can be identified, and the peak height can be utilized to estimate the concentrations of each element [32, 33].

Antibacterial assay - Disc diffusion test

ZnO NPs antibacterial activity was tested using the disc diffusion method against two types of bacteria, including *Escherichia coli (ATCC 25922)* and *Staphylococcus aureus (ATCC 29737)*. After incubating overnight cultural samples in Mueller Hinton Agar (100 mL), wells were made on the agar plates using a sterile polystyrene tip (4 mm). 20 μg mL^{-1} of fresh ZnO NPs were separately prepared and utilized in the assay. To determine the antibacterial activity, the diameter of the inhibition zone around the well was measured.

Antioxidant assay – DPPH test

adical scavenging activity can be measured by a standard method using DPPH (2,2-diphenyl-1-picrylhydrazyl). The DPPH method uses antioxidants that react with stable DPPH* (deep violet color) and then alter it into 2,2-diphenyl-2-picrylhydrazine (DPPH:H) that shows yellow discoloration [34]. For assessment, 500 μl of 1M DPPH solution dissolved with 100% methanol was added to various concentrations of *p. vera* peel extract-mediated ZnO NPs (12.5-250 μg ml^{-1}). For 40 minutes, the mixture was incubated in the dark after being shaken vigorously. During the study, Ascorbic acid was present as a positive control. Analyzing the absorbance of the reactant at OD517 nm was performed after incubation. As a result, the DPPH scavenging activity of ZnO NPs synthesized by *p.vera* peel extract was compared with that of Ascorbic acid.

Using the formula below, we calculated the percentage of free radical scavenging activity (RSA):

$$RSA\ (\%) = [(A_{control} - A_{sample})/A_{control}] \times 100 \quad (1)$$

Where:

$A_{control}$ = absorbance of DPPH without sample

A_{sample} = absorbance of DPPH with sample

Catalytic activity

To assess the catalytic property of ZnO NPs in wastewater treatment, 30 ml (15 mg L^{-1}) of textile wastewater contaminated by MB was provided. 5 mg of $NaBH_4$ (Merck®) as a reducing agent in this reaction was added to the dye solution at a basic pH equal to 10 at room temperature. Different concentrations (20, 40, 60, 80, and 100 mg) of ZnO nanocatalyst were used to determine the optimal catalyst concentration. The absorbance of methylene blue was recorded every 30 seconds through the UV-VIS spectrometer (Shimadzu UV-160A) between 400 and 800 nm to study the reduction of the organic dye by ZnO NPs.

Photocatalytic activity

By using a nanocatalyst and MB dye, we determined the photocatalytic activity of green synthesized ZnO NPs in an isolated box containing a 10 W UV lamp (Merck Millipore) that irradiated the 30 ml glass balloon. By adding 100 mg of nanocatalyst to 30 ml of 10 mg L^{-1} MB solution, photocatalytic degradation was initiated. The solution was stirred mechanically by a cylindrical magnetic stirring bar, and by measuring the UV-VIS absorption intensity in the 200–800 nm range every 2 minutes, the MB concentration was determined. In addition, five different concentrations of nanocatalyst between 20 and 100 mg were tested in order to determine the optimal concentration.

In order to estimate dye degradation in both catalytic and photocatalytic assay [13], the following formula was used:

$$\%Decolorization = 100 \times \frac{(C_0 - C)}{C_0} \quad (2)$$

C_0 represents the initial concentration of dye solution, and C represents the concentration of dye solution after organic dye degradation.

RESULTS AND DISCUSSION

UV-Vis analysis

In order to determine the optical properties of the prepared ZnO NPs, UV-visible spectroscopy analysis was performed. ZnO NPs synthesized from *pistachio vera* skin extract, like many other nanoparticles, exhibit a UV-vis band between 380 nm and 440 nm, which is within the ZnO NPs range (Figure 2a) [35]. As a result of the absorption of a photon and the excitation of an electron from the valence band into the electron/hole pair formed by the conduction band, visible absorption occurs [36, 37]. It was determined that the band gap is 2.89 eV through the use of a Tauc plot calculation (Figure 2b).

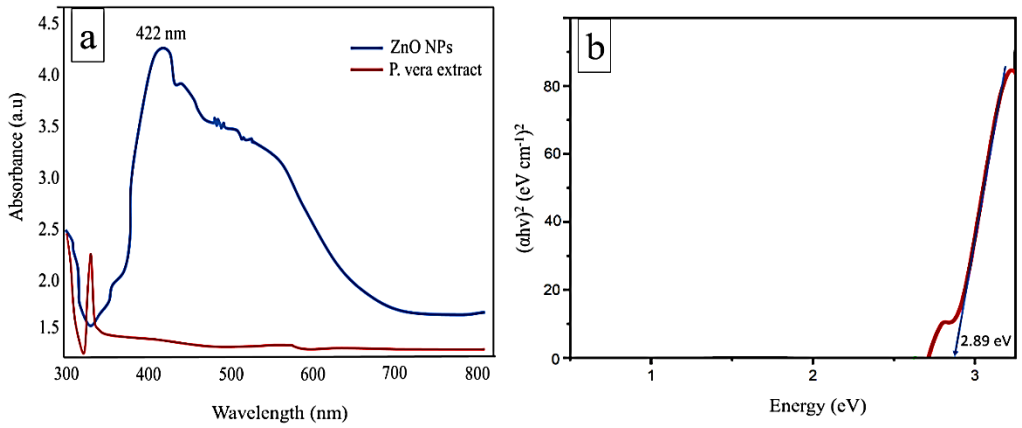

Figure 2. UV-vis spectrum of ZnO nanoparticle and *P. vera* peel extract (a) Tauc's plots for the energy band gap (b)

Fourier-transform infrared spectroscopy (FTIR)

The FTIR spectrum shows the environment-friendly ZnO NPs mediated by extract of the *p.vera* peel was successfully formed. Due mainly to flavonoid (polyphenol) compounds and protein molecule stabilization, the peak at 500 cm^{-1} is related to Zn-O formation (Figure 3). The broadest peak in the spectrum, at 3490 cm^{-1}, is equal to the stretching of O-H and (or) N-H in amino acids, phenols, and alcohols. The peak of 1537 cm^{-1} is associated with C=C tension in ketones. Moreover, the peak at 1397 cm^{-1} is related to C=O tension. The peaks at 1045 cm^{-1} relates to carbohydrate (C-O), and the next peak at 612 cm^{-1} could be appointed to C-H bending. Biomolecules, such as terpenoids, synthesize nanoparticles containing alcohols, ketones, aldehydes, and carboxylic acids as functional groups.

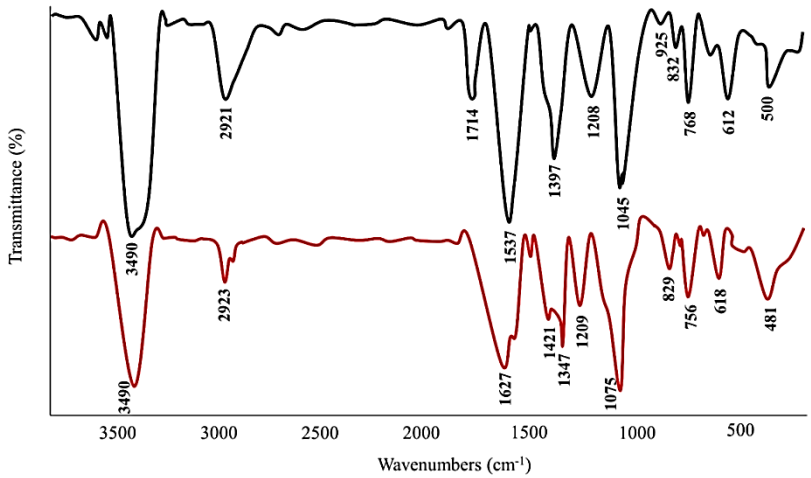

Figure 3. Zinc Oxide nanoparticles (black) and *P. vera* peel extract (red) FTIR spectra

Based on FTIR analysis, they have a strong capability in phenolic metal bonding. ZnO NPs are formed when the functional groups of *P. vera* soft peel extract donates reducing electrons to Zn^{2+} that reduce it to Zn^{0}. ZnO NPs formation can also be stabilized by these functional groups [38].

XRD

The related face velocities and crystal symmetry of ZnO give the compound a hexagonal common crystal structure. Additionally, ZnO NPs also include thermodynamically stable crystallographic phases. A quantum size effect increases the peaks' width in ZnO NPs. It is estimated that the average particle size was obtained at 42 nm via the Scherer equation. Eight intense diffraction peaks were displayed by the XRD pattern (Figure 4), including (100), (002), (101), (102), (110), (103), (112), and (201) at 2θ values of 31°, 34°, 35.6°, 47°, 56°, 62.5°, 66.2°, and 68.3°, respectively. The XRD pattern and the data reported in the present study follow the Joint Committee on Powder Diffraction Standards (JCPDS, card No. 36-1451). In addition, Polycrystalline ZnO NPs structures can be seen in the peak at (101) [39].

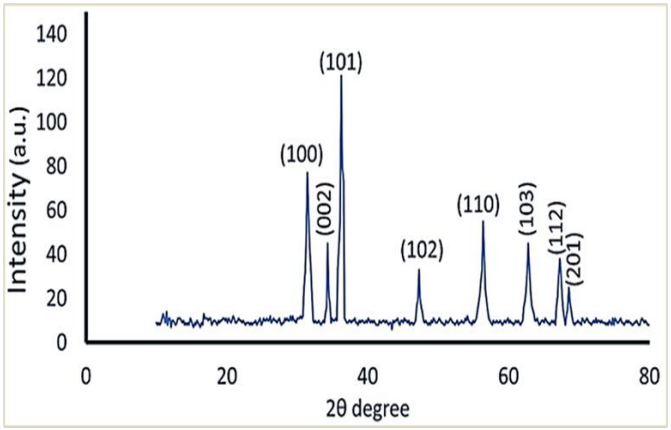

Figure 4. XRD pattern of synthesized ZnO NPs

SEM

The morphology of ZnO NPS was studied using scanning electron microscopy (SEM) (Figure 5). XRD analysis information can be verified by inspecting the size of the nanoparticles in these images [40]. According to the Figures, the particles were formed by the oval structure and quasi-spherical formation. SEM images substantiate the Scherrer equation results in the XRD analysis section. The size range of the particles is between 31.14 and 48 nm with an average of 42 nm. As shown in the images, the particles also appear inclined together, which is caused by the presence of a stable capping agent.

EDX

Figure 6 illustrates the results of the use of energy dispersive X-ray spectroscopy (EDX) to investigate the chemical composition of biosynthesized ZnO NPs. In the EDX spectrum, only Zn and O peaks are observed, indicating that the zinc and oxygen stoichiometric values are identical in ZnO NPs [41]. According to stoichiometric theory, Zn and O should contain 80.3% and 19.7% mass percent, respectively. As a result of the high purity of the synthesized hexagonal ZnO, there are no stray peaks in the EDX spectrum. Based on XRD patterns and EDX spectra, the hexagonal ZnO nanoparticles are exclusively composed of Zn and O atoms.

Antibacterial activity

Bacteria are microscopic, single-celled organisms that live in almost every environment on Earth, from deep-sea vents to the guts of humans. The microorganisms are highly resilient. They spread quickly and can adapt to a wide range of environmental conditions, causing generally adverse health effects on human beings [42, 43]. By using plant extracts to produce ZnO NPs, it is possible to prevent bacterial biofilms from forming, which leads to a rise in antibiotic resistance.

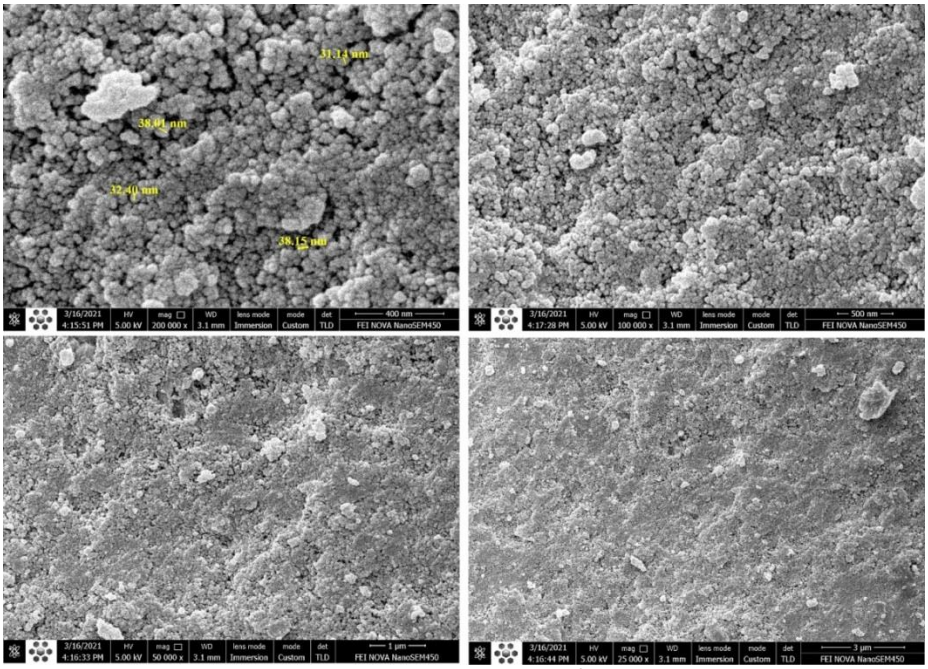

Figure 5. Scanning electron microscopy (SEM) image of *P. vera*-mediated ZnO NPs

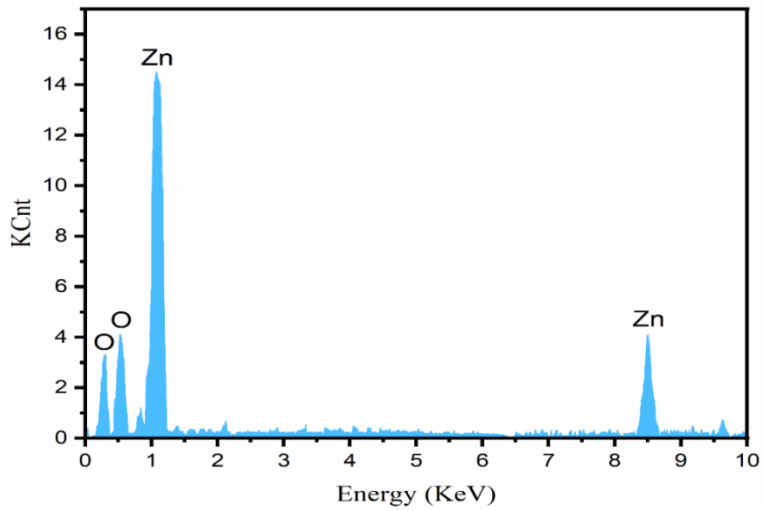

Figure 6. Energy Dispersive X-ray (EDX) analysis of ZnO NPs.

These NPs have good antibacterial properties, biocompatibility, safety, and stability, which will create a new research area in the field of antibacterial agents [44-46]. *E. coli* and *S. aureus* cells' growth was attenuated by phyto-synthesised ZnO NPs caused by the interaction with the bacterial velum. Antibacterial properties of ZnO nanoparticles are attributable to oxidative stress caused by reactive oxygen species formed on their surfaces, which causes bacterial membrane rupture. These molecules contain oxygen, perhydroxyl radicals, superoxide anion, and hydroxyl radicals capable of destructively destroying DNA and RNA, and oxidizing proteins and lipids, thus causing bacterial death [47]. Figure 7 exhibits the mechanism of bacteria cell death by green synthesized ZnO NPs, where the DNA, cell membrane, mitochondria, and essential proteins confront formidable damages.

The assay was performed using the agar disc diffusion method. The antibacterial effect of ZnO NPs was visualized against urinary tract infection pathogens. Whole tests were conducted in triplicate. In-vitro antibacterial activities demonstrate that zinc oxide NPs synthesized by *P. vera* peel extract prevent bacteria growth. An explanation for ZnO NPS's antimicrobial efficacy may be *P. vera* peel extract, which functions as a capping agent, and by reducing particle size, enhances antimicrobial activity. This is due to smaller particles typically having a higher surface-to-volume ratio, which

makes them more efficient antibacterial agents [48, 49]. The inhibition zone made by ZnO NPs grows up to 20 mm for *E. coli*, and up to 24 mm for *S. aureus*, as displayed in Table 1. Green synthesized ZnO NPs have been shown in comparison with the control sample to be an extremely promising candidate as a safe and environmentally friendly antimicrobe.

Table 1. Inhibition zone of ZnO NPs and control sample.

Bacterial strain	Inhibition zone (mm)	
	ZnO NPs	Tetracycline 20 µg mL^{-1}
Escherichia coli	20	24
Staphylococcus aureus	24	26

Antioxidant activity

A substance considered an antioxidant exists at low concentrations relative to an oxidizable substrate and noticeably delays or inhibits the oxidation of that stratum [50].

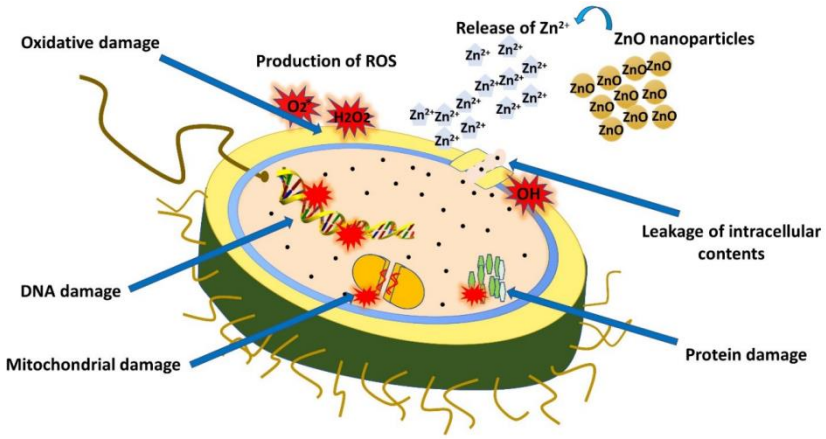

Figure 7. A common mechanism of bacterial inhibition by ZnO NPs biosynthesized by *P. vera* peel extract

Antioxidants are used for treating a wide array of illnesses. Several studies based on standard in vitro methods demonstrate that ZnO NPs are also potent antioxidants [51]. In the presence of an antioxidant (radical scavenger), the DPPH radical is reduced to DPPH-H (yellow) by either accepting a hydrogen atom or an electron (Figure 8). DPPH turns light yellow when its odd electron is paired off with a free radical scavenger, resulting in a decolorization. As the color of DPPH changes, the scavenging activity of the synthesized ZnO is determined spectrophotometrically [52]. The radical scavenging activity (%) of the prepared ZnO is calculated using Eq (1).

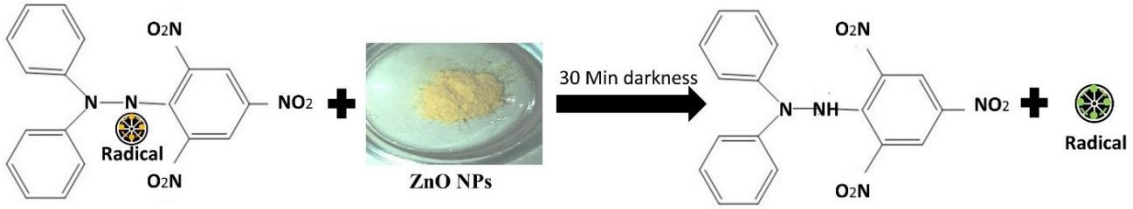

Figure 8. Mechanism of radical scavenging activity by ZnO NPs (DPPH* to DPPH:H (yellow)).

The standard in-vitro DPPH assay demonstrates that *P. vera* peel extract-mediated ZnO NPs are a significant competitors of common antioxidants known in medical areas. As exhibited in Figure 9 and Table 2, diverse dosage (12.5-250 µg/ml) of ZnO NPs was utilized in the DPPH test. The dosage of 100 µg mL^{-1} ZnO NPs showed

the highest antioxidant activity. Conversely, Ascorbic acid, known as a solid antioxidant, demonstrate lower radical scavenging activity at the exact dosage. The radical scavenging property of ZnO NPs decreases with dosage increment, whereas Ascorbic acid RSA % increases. The antioxidant characteristics of ZnO could be due to the phytochemicals coated on them derived from the aqueous peel extracts [53]. Plant phytochemicals, in particular polyphenols, can donate hydrogen atoms to reduce DPPH* to DPPH:H when they attach to their OH groups [54, 55]. Furthermore, it may be possible for synthesized ZnO to have scavenging activity due to the presence of oxygen electron density over nitrogen electron density in DPPH [56]. Consequently, the radical scavenging activity of phytogenic synthesized ZnO may depend upon factors such as the concentration and the number of phytochemicals coated on its surface [57].

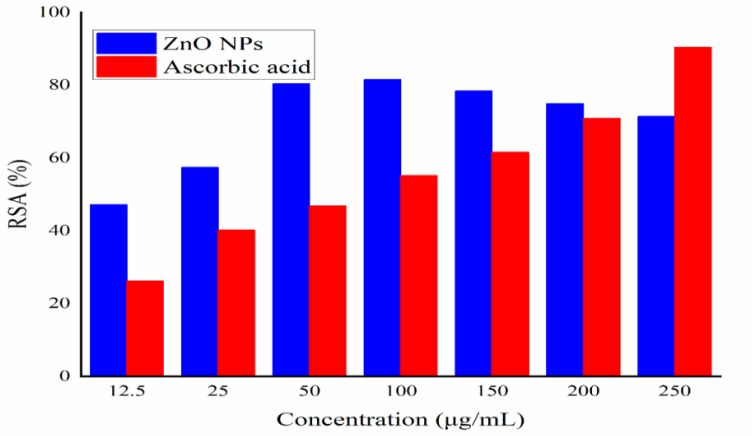

Figure 9. DPPH scavenging activity of ZnO NPs in comparison to Ascorbic acid.

Table 2. DPPH scavenging activity of ZnO NPs and Ascorbic acid

Concentration (µg mL^{-1})	DPPH inhibition activity (%)	
	ZnO NPs	Ascorbic acid
12.5	47.16981	26.18745
25	57.41768	40.17454
50	80.39216	46.78541
100	81.57603	55.14587
150	78.43137	61.58474
200	74.95376	70.87458
250	71.47614	90.45785

Dye reduction by $NaBH_4$

The removal of methylene blue by the biosynthesized ZnO nanocatalyst was reduced by $NaBH_4$ and monitored by the UV-Vis spectrophotometer. Even though $NaBH_4$ does not exhibit any catalytic activity in MB solution, different concentrations of ZnO NPs cause a color change that is evident. The optimal concentration of nanocatalyst was determined using different concentrations of nanocatalyst in the same pH and dye concentration. As shown in Figure 10, the highest catalytic activity of ZnO NPs emerged at 60 mg. On the other hand, as the concentration of nanoparticles increases (80 and 100 mg), the catalytic activity declines. Therefore, 60 mg was selected as the optimum dose of ZnO nanocatalyst for the main dye reduction study.

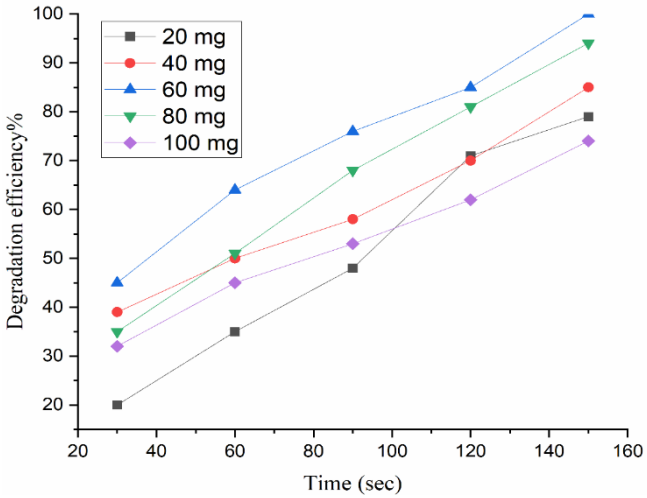

Figure 10. Concentration effect on MB degradation activity of ZnO NPs.

By using the optimum concentration of ZnO NPs, MB dye was eliminated in 150 seconds (Figure 11). Equation 1 was used to calculate the final dye degradation percentage, which is 100%. Hence, ZnO nanocatalyst biosynthesized by *P. vera* soft peel extract exhibits high catalytic activity in organic dye degradation while conforming to all principles of green chemistry.

Methylene blue reduction mechanism

Regarding the more ecological side of catalytic processes, developing environmentally friendly procedures, preferably in aqueous environments, is highly desirable. Avoiding the use of volatile organic solvents; sodium borohydride ($NaBH_4$) is one of the preferred water-soluble reducing agents for representative reductions. Following the effect of electron transfer, the organic color reduction reaction can be justified. ZnO, as a well-known semiconductor, can effectually transfer electrons between receptors and donors. Consequently, electrons will be transferred to the receptor (MB) with the help of the donor (BH_4^-). This process converts methylene blue to leucomethylene blue [58, 59].

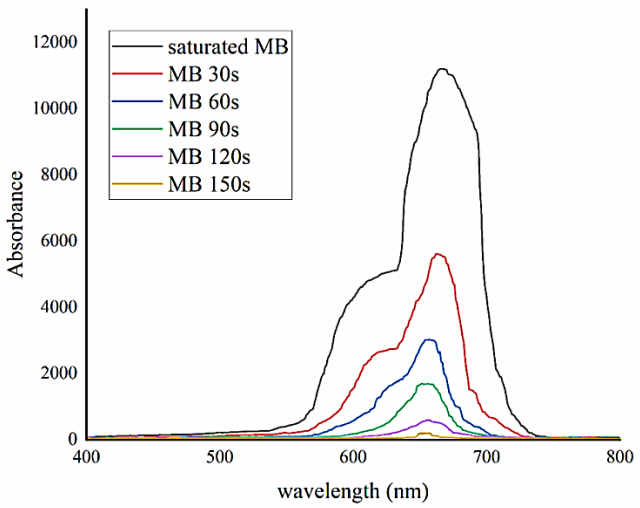

Figure 11. Successive reduction of MB by ZnO NPs in the presence of $NaBH_4$

Photocatalytic dye degradation

We investigated the photocatalytic activity of ZnO nanocatalysts using methylene blue at a fixed concentration and a constant pH. In order to estimate the potential catalytic activity of UV radiation, two different

MB solutions were studied in the absence and presence of ZnO NPs. Passing over 30 minutes; it was observed that the MB solution concentration did not vary in the absence of ZnO. Thus, this indicates that UV light alone does not decompose the organic dye and that ZnO nanocatalysts can decompose MB. Moreover, five different nanocatalyst concentrations were tested between 20 and 100 mg in order to determine the optimal concentration. Based on the results of this study, as well as the results of the catalytic activity test, 60 mg is the optimal nanocatalyst concentration for MB removal (Figure 12).

The nanoparticles designed in this study were capable of decomposing and removing MB from aqueous media within 14 minutes (Figure 13). Physicochemical properties of nanoparticles and their low band gap may contribute to this result. Using equation 1, we calculated the percentage of color degradation, which equals 98%.

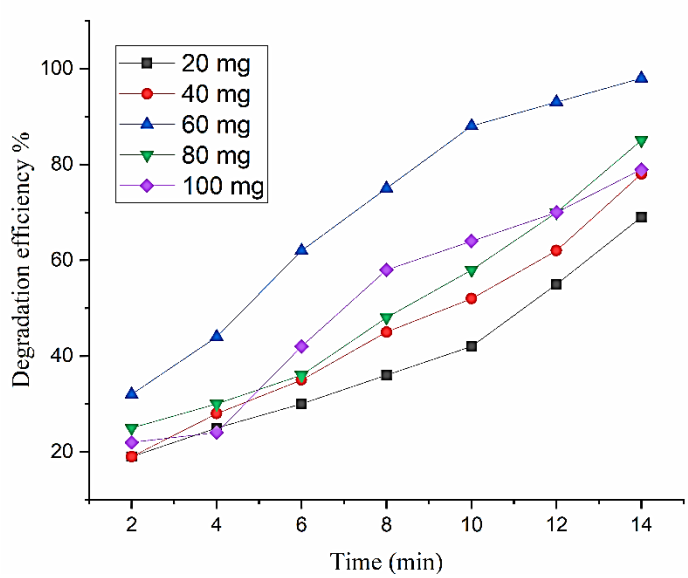

Figure 12. Concentration effect on MB degradation activity of ZnO NPs

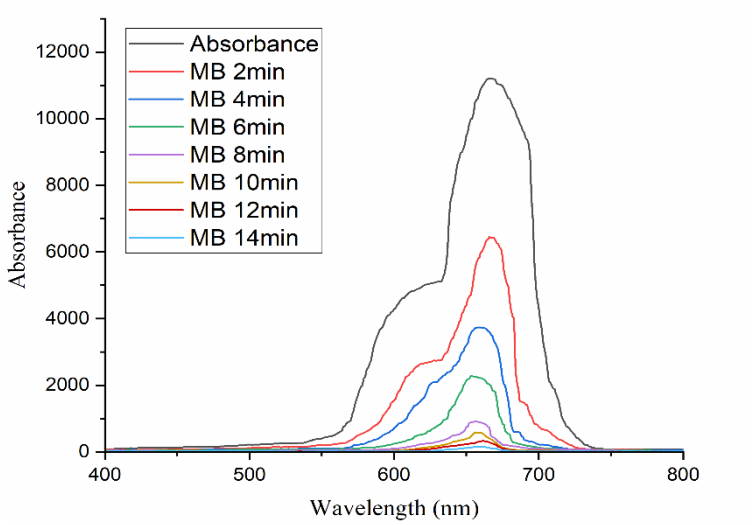

Figure 13. Successive photodegradation of MB by ZnO NPs

Methylene blue photodegradation mechanism

ZnO is a good choice for photocatalytic applications due to its high photocatalytic activity and optical properties. As the photocatalytic reaction is a form of molecular excitation of the photocatalyst, it is often called a photo-induced reaction. Photocatalytic degradation occurs through chemical reactions. The initiation stage of the reaction is the creation of an electron-hole pair. The photocatalytic reaction occurs when a photon of sufficient wavelength induces molecular excitation of the photocatalyst. The chemical process of molecule

excitation contributes to electrons switching from the valence band level (vbl) to the conduction band level (cbl) and the creation of holes within the valence band level (vbl) [13]. In other words, when illuminated by light stronger than the band gap energy, the electron-hole pairs diffuse into the photocatalyst surface and participate in the chemical reaction. As a result of significant super-strong oxidation, certain free electrons and holes are capable of converting the surrounding oxygen or water molecules into highly reactive and unstable free radicals. Accordingly, Zn^{+2} ions must be the most abundant of all zinc species present in aqueous dye solutions under the experimental conditions, followed by $Zn(OH)^{+}$,$Zn(OH)_3^{-}$, and $Zn(OH)_4^{2-}$ [60, 61]. A schematic representation of the process is shown in Figure 14 for a better understanding of the mechanisms and reactions.

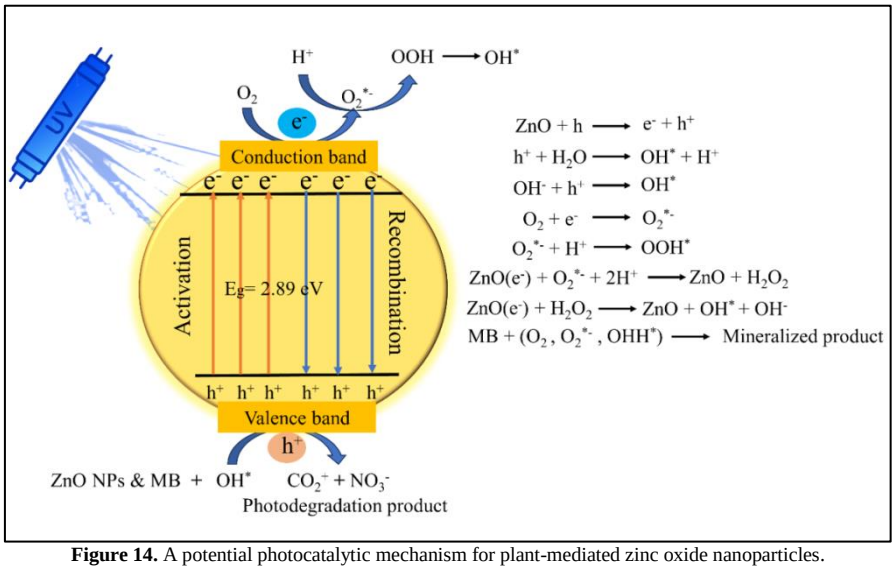

Figure 14. A potential photocatalytic mechanism for plant-mediated zinc oxide nanoparticles.

Catalyst stability

The use of a catalyst in large quantities demands both great activity and stability. To determine the effectiveness of their recycling, ZnO NPs were reused to degrade the MB dye over four consecutive cycles. Used nanoparticles were washed with distilled water and dried at 90ºC in order to prepare them for reuse. Catalytic activity was not significantly reduced following several degradation cycles. As well, the nanoparticles in this study did not change significantly over a period of four consecutive cycles of exposure to ultraviolet rays, and their performance remained the same.

In general, this study showed that by using plant components extracts such as fruit peels extract, fully functional nanoparticles of plant origin can be biosynthesized. Since this synthesis follows all the green chemistry principles, the produced nanoparticles can be called green and environmentally friendly nanoparticles. Considering the properties and application of nanoparticles produced in this study, as well as their recycling properties, they can be used in industry and medical and pharmaceutical applications. Due to their physicochemical properties, nanoparticles possess significant catalytic and photocatalytic properties that are competitive with other methods of purifying water contaminated with organic dyes. Research on other organic dyes will allow us to better understand how these nanoparticles can be utilized in the treatment of water contaminated with other dyes or multiple dyes, and if necessary, positive changes can be made to optimize these nanoparticles. The important point in these syntheses is to identify the effective factors in the synthesis and properties of nanoparticles, which by studying more in this field, it is possible to produce nanoparticles that are completely competitive with other chemical materials.

CONCLUSIONS

The peel extract of *Pistacia vera* was used for the first time to synthesize ZnO NPs by green chemistry

approach. ZnO NPs can be produced quickly, efficiently, and simply by using a fast biological pathway with plant waste peel extract. The spherical prepared ZnO NPs were characterized utilizing FTIR, XRD, EDX, UV-Vis absorption and SEM techniques. Based on the SEM images, the nanoparticles are mostly oval and quasi-spherical within the diameter range of 31.14 to 48 nm. According to FTIR, the peak at 500 cm^{-1} is the typical absorption of the Zn-O bond, confirming the ZnO NPs formation. The formation of a hexagonal wurtzite phase is confirmed by X-ray diffraction. At ambient temperatures, it is the most stable form of zinc oxide. This procedure is an economical technique to prepare nanocrystalline zinc oxide based on time, energy, and simplicity. The disc diffusion technique against clinical strains of *Escherichia coli* and *Staphylococcus aureus* demonstrates that ZnO NPs are remarkable antibacterial candidates. In addition, the radical scavenging method, the DPPH test, shows that ZnO NPs have striking antioxidative activity and can successfully discolor unstable DPPH. The multi-functional nanocatalyst biosynthesized by *Pistacia vera* soft peel extract reduces methylene blue as an organic pollutant dye in 150 seconds, which is a significant improvement in the catalytic activity of ZnO NPs. Furthermore, these nanoparticles have the ability to decompose MB in 14 minutes under ultraviolet light. As a result of these nanoparticles' properties and the methods used in their synthesis, which are based on plant waste, by completing more extensive studies in the future, they can be used in various industries and contribute to preserving the environment and advancing green chemistry science.

ACKNOWLEDGEMENTS

Authors are thankful to the Department of Chemistry and deputy of research of Qom University of Technology for technical support in this project.

Conflicts of interest

All authors declare that there is no conflict of interest.

Funding

As of the time this manuscript was being prepared, no funds, grants, or other support were received by the authors.

Financial interest

Neither of the authors discloses relevant financial or non-financial interests related to this article.

Author Contributions

The manuscript was written through contributions of Hossein Gholchinpour, Alireza Momeni and Mohammad Hadi Meshkatalsadat . The final version of the manuscript has been approved by the authors.

Conflict of interests

There is no relevant financial or non-financial interest to disclose by the authors.

Research Data Policy and Data Availability

The datasets generated during and/or analysed during the current study are available from the corresponding author on reasonable request.

REFERENCES

1. Xu J., Huang Y., Zhu S., Abbes N., Jing X., Zhang L., 2021. A review of the green synthesis of ZnO nanoparticles using plant extracts and their prospects for application in antibacterial textiles. Journal of Engineered Fibers and Fabrics. 16, 1-14, https://doi.org/10.1177/15589250211046242

2. Saif, S., Tahir, A., Asim, T., Chen, Y., Khan, M., Adil, S.F., 2019. Green synthesis of ZnO hierarchical microstructures by Cordia myxa and their antibacterial activity. Saudi J Biol Sci. 26, 1364–1371. https://doi.org/10.1016/j.sjbs.2019.01.004

3. Ahmed S., Chaudhry S.A., Ikram S., 2017. A review on biogenic synthesis of ZnO nanoparticles using plant extracts and microbes: a prospect towards green chemistry. J Photochem Photobiol B Biol. 166, 272–284. https://doi.org/10.1016/j.jphotobiol.2016.12.011

4. Velsankar K, Sudhahar S and Maheshwaran G., 2019. Effect of biosynthesis of ZnO nanoparticles via Cucurbita seed extract on Culex tritaeniorhynchus mosquito larvae with its biological applications. J Photochem Photobiol B Biol. 200, 111650.

https://doi.org/10.1016/j.jphotobiol.2019.111650

5. Shabaani M., Rahaiee S., Zare M., Jafari S.M., 2020. Green synthesis of ZnO nanoparticles using loquat seed extract; biological functions and photocatalytic degradation properties. LWT. 134, 110133. https://doi.org/10.1016/j.lwt.2020.110133

6. Güy N., Özacar M., 2016. The influence of noble metals on photocatalytic activity of ZnO for Congo red degradation. Int J Hydrogen Energy. 41(44), 20100–20112. https://doi.org/10.1016/j.ijhydene.2016.07.063

7. Podasca V.E., Buruiana T., Buruiana E.C., 2016. UV-cured poly- meric films containing ZnO and silver nanoparticles with UV–vis light-assisted photocatalytic activity. Appl Surf Sci. 377, 262–273. https://doi.org/10.1016/j.apsusc.2016.03.178

8. Sohrabnezhad S., Seifi A., 2016. The green synthesis of Ag/ ZnO in montmorillonite with enhanced photocatalytic activ- ity. Appl Surf Sci. 386, 33–40. https://doi.org/10.1016/j.apsusc.2016.05.102

9. Zubair N., Akhtar K., 2020. Morphology controlled synthesis of ZnO nanoparticles for in-vitro evaluation of antibacte- rial activity. Trans Nonferrous Met Soc China. 30(6), 1605–1614. https://doi.org/10.1016/S1003-6326(20)65323-7

10. Wang L., Kang Y., Liu X., Zhang S., Huang W., Wang S., 2012. ZnO Nanorod Gas Sensor for Ethanol Detection. Sensors & Actuators, B: Chemical. 162, 237-243. http://dx.doi.org/10.1016/j.snb.2011.12.073

11. Cross S.E., Innes B., Roberts M.S., Tsuzuki T., Robertson T.A., McCormick P., 2007. Human Skin Penetration of Sunscreen Nanoparticles: In-Vitro Assessment of a Novel Mi- cronized Zinc Oxide Formulation. Skin Pharmacology and Physiology. 20, 148-154. http://dx.doi.org/10.1159/000098701

12. Park J.K., Rupa E.J., Arif M.H., Li J.F., Anandapadmanaban G., Kang J.P., Kim M., Ahn J.C., Akter R., Yang D.C., Kang S.C., 2021. Synthesis of zinc oxide nanoparticles from Gynostemma pentaphyllum extracts and assessment of photocatalytic properties through malachite green dye decolorization under UV illumination-A Green Approach. Optik, 239. pp.166249. https://doi.org/10.1016/j.ijleo.2020.166249

13. Umar K., Mfarrej M.F.B., Rahman Q.I., Zuhaib M., Khan A., Zia Q., Banawas S., Nadeem H., Khan M.F., Ahmad F., 2022. ZnO Nano-swirlings for Azo Dye AR183 photocatalytic degradation and antimycotic activity. Scientific Reports. 12(1), 14023. https://doi.org/10.1038/s41598-022-17924-3

14. Meshkatalsadat M.H., Momeni A., Abdollahzadeh M.R., 2023. Biosynthesis of Zinc Oxide Nanoparticles Using Punica granatum L. Waste Peel Extract, and Assessment of Antioxidant and Catalytic Activity. Nano Biomedicine and Engineering.

15. Zhou J., Xu N., Wang Z.L., 2006. Dissolving Behavior and Stability of ZnO Wires in Biofluids: A Study on Biodegradability and Biocompatibility of ZnO Nanostructures. Ad- vanced Materials. 18, 2432-2435. http://dx.doi.org/10.1002/adma.200600200

16. Rasmussen J.W., Martinez E., Louka P., Wingett D.G., 2010. Zinc Oxide Nanopar- ticles for Selective Destruction of Tumor Cells and Potential for Drug Delivery Applica- tions. Expert Opinion on Drug Delivery. 7, 1063-1077.

17. Padalia H., Moteriya P., Chanda S., 2018. Synergistic antimicrobial and cytotoxic potential of zinc oxide nanoparticles synthesized using *Cassia auriculata* leaf extract. Bionanoscience. 8(1), 196–206. https://doi.org/10.1007/S12668-017-0463-6

18. Akbarian M., Mahjoub S., Mohammad S., Zabihi E., 2020. Biointerfaces Green synthesis, formulation and biological evaluation of a novel ZnO nanocarrier loaded with paclitaxel as drug delivery system on MCF-7 cell line. Colloids Surf B Biointerfaces. 186, 110686. https://doi.org/10.1016/j.colsurfb.2019.110686

19. Chen L., Batjikh I., Hurh J., Han Y., Huo Y., Ali H., Li J.F., Rupa E.J., Ahn J.C., Mathiyalagan R., Yang D.C., 2019. Green synthesis of zinc oxide nanoparticles from root extract of Scutellaria baicalen- sis and its photocatalytic degradation activity using methylene blue. Optik (stuttg). 184, 324–329.

20. Elumalai K., Velmurugan S., Ravi S., Kathiravan V., Ashokkumar S., 2015. Green synthesis of zinc oxide nanoparticles using Moringa oleifera leaf extract and evaluation of its antimicrobial activity. Spectrochim Acta A. 143, 158–164.

21. Rajamanickam U., Mylsamy P., Viswanathan S., Muthusamy P., 2012. Biosynthesis of zinc nanoparticles using actinomycetes for antibacterial food packaging, in Proceedings of the International Conference on Nutrition and Food Sciences (IPCBEE ’12). vol. 39.

22. Nithya M., Kalyanasundharam S., 2018. Effect of chemically synthesis compared to biosynthesized ZnO nanoparticles using aqueous extract of C. halicacabum and their antibacterial activity, OpenNano. https://doi.org/10.1016/j.onano.2018.10.001

23. Tavallali V., Rahemi M., 2007. Effects of Rootstock on Nutrient Acquisition by Leaf, Kernel and Quality of Pistachio (*Pistacia vera* L.) American-Eurasian J Agric & Environ. Sci. 2(3), 240–246, 240.

24. Clara D. A., Rajeswari V., Sathyajothi S., 2017. Green synthesis of zinc oxide nanoparticle using green tea leaf extract for supercapacitor application. Materials Today. 4, 660–667. https://doi.org/10.1016/j.matpr.2017.01.070

25. Feng S., Aijun Y., Dong M.Y., JuanW., Xue G., Hong X.T., 2018. Biosynthesis of Barleria gibsoni leaf extract mediated zinc oxide nanoparticles and their formulation gel wound therapy in nursing care of infants and children. Journal of Photochemistry and Photobiology. B.

26. Agarwal H., Menon S., Venkat K.S., Rajeshkumar S., David S.R., Lakshmi T., Deepak N.V., 2019. Phyto-assisted synthesis of zinc oxide nanoparticles using Cassia alata and its antibacterial activity against *Escherichia coli.* Biochemistry and Biophysics Reports. 17, 208–211. https://doi.org/10.1016/j.bbrep.2019.01.002

27. Rathod T., Padalia H., Chanda S., 2017. Green synthesized zinc oxide nanoparticles as a therapeutic tool to combat candidiasis. AIP Conf. Proc. 1837(1), 040065. https://doi.org/10.1063/1.4982149

28. Gupta M., Tomar R.S., Kaushik S., Mishra R.K., Sharma D., 2018. Effective antimicrobial activity of green ZnO nano particles of Catharanthus roseus. Frontiers in Microbiology. 9, 1–13. https://doi.org/10.3389/fmicb.2018.02030

29. Alejandro E., Silvio A.M., Rodriguez-Paez J.E., 2019 Synthesis of ZnO nanoparticles with different morphology: Study of their antifungal effect on strains of Aspergillus niger and Botrytis cinerea. Materials Chemistry and Physics. 234, 172–184. https://doi.org/10.1016/J.MATCHEMPHYS.2019.05.075

30. Mona H., Saba H., Kambiz V., Hojat V., 2018. Green synthesis, antibacterial, antioxidant and cytotoxic effect of gold nanoparticles using Pistacia Atlantica extract. Journal of Taiwan Institute of Chemical Engineers. 1, 1–10. https://doi.org/10.1016/j.jtice.2018.07.018

31. Sekar V., Baskaralingam V., Balasubramanian M., Malaikkarasu S., 2016. Laurus nobilis leaf extract mediated green synthesis of ZnO nanoparticles: characterization and biomedical applications. Biomedicine & Pharmacotherapy. 84, 1213–1222. https://doi.org/10.1016/j.biopha.2016.10.038

32. Brożek-Mucha Z., 2014. On the prevalence of gunshot residue in selected populations - an empirical study performed with SEM-EDX analysis. Forensic Sci Int. 237, 46-52.

33. Simone Bischetti M.S., Kaur Lamsira H., Bonfiglio R., Bonanno E., 2018. Energy Dispersive X-ray (EDX) microanalysis: A powerful tool in biomedical research and diagnosis. Eur J Histochem. 62(1), 2841. https://doi.org/10.4081/ejh.2018.2841

34. Du L., S. Suo G. Wang, 2013. Mechanism and cellular kinetic studies of the enhancement of antioxidant activity by using surface-functionalized gold nanoparticles," Chemistry A: European Journal.vol. 19(4), 1281–1287. https://doi.org/10.1002/chem.201203506

35. Patiño-Portela C., Guerra–Sierra B. E., Muñoz-Florez J. E., Rodríguez-Páez J.E., 2020. Antifungal effect of zinc oxide nanoparticles on Colletotrichum sp., causal agent of anthracnose in coffee crops, Biocatalysis and Agricultural Biotechnology. 25, 101579. https:// doi.org/ 10.1016 / j.bcab.2020.101579

36. Parveen S., Wani A.H., Shah M.A., Devi H.S., Bhat M.Y., Koka J.A., 2018. Preparation, characterization and antifungal activity of iron oxide nanoparticles. Microbial pathogenesis. 115, 287-292. https://doi.org /10.1016/j.micpath.2017.12.068

37. Kumar S.A., Jarvin M., Inbanathan S.S.R., Umar A., Lalla N.P., Dzade N.Y., Algadi H., Rahman Q.I., Baskoutas S., 2022. Facile green synthesis of magnesium oxide nanoparticles using tea (Camellia sinensis) extract for efficient photocatalytic degradation of methylene blue dye. Environmental Technology & Innovation. 28, p.102746. https://doi.org/10.1016/j.eti.2022.102746

38. Ezealisiji K.M., Siwe-Noundou X., Maduelosi B., Nwachukwu N., Krause R.W.M., 2019. Green synthesis of zinc oxide nanoparticles using *Solanum torvum* (L) leaf extract and evaluation of the toxicological profile of the ZnO nanoparticles–hydrogel composite in Wistar

albino rats. International Nano Letters. 9, 99-107. https://doi.org/10.1007/s40089-018-0263-1

39. Monshi A., Foroughi M.R., Monshi M.R., 2012. Modified Scherrer equation to estimate more accurately nano-crystallite size using XRD. WorldJ Nano Sci Eng. 2, 154–160 https://doi.org/10.4236/wjnse.2012.23020

40. Rahman Q.I., Ali A., Ahmad N., Lohani M.B., Mehta S.K., Muddassir M., 2020. Synthesis and characterization of CuO rods for enhanced visible light driven dye degradation. Journal of Nanoscience and Nanotechnology. 20(12), 7716-7723.

41. Rahman Q.I., Ahmad M., Misra S.K., Lohani M.B., 2013. Hexagonal ZnO nanorods assembled flowers for photocatalytic dye degradation: Growth, structural and optical properties. Superlattices and Microstructures. 64, 495-506. https://doi.org/10.1016/j.spmi.2013.10.011

42. Barry R. Bochner, 2009. Global phenotypic characterization of bacteria, FEMS Microbiology Reviews. 33(1), 191–205. https://doi.org/10.1111/j.1574-6976.2008.00149.x

43. Rogers K., Kadner Robert J., 2020. bacteria. Encyclopedia Britannica. https:// www.britannica. com/science/bacteria.

44. Awwad A.M., Amer M.W., Salem N.M., Abdeen A.O., 2020. Green synthesis of zinc oxide nanoparticles (ZnO-NPs) using Ailanthus altissima fruit extracts and antibacterial activity. Chem Int. 6.3, 151-159 https://doi.org/10.5281/zenodo.3559520

45. Debjani B., Shivapriya P.M., Kumar Gautam P., Misra K., Sahoo A.K., Samanta S.K., 2020. A Review on Basic Biology of Bacterial Biofilm Infections and Their Treatments by Nanotechnology-Based Approaches" Proceedings of the National Academy of Sciences, India, Section B: biological sciences. 90(2), 243-259. https://doi.org/10.1007/s40011-018-01065-7

46. Anand G.T., Renuka D., Ramesh R., Anandaraj L., Sundaram S.J., Ramalingam G., Kaviyarasu K., 2019. Green synthesis of ZnO nanoparticle using *Prunus dulcis* (almond gum) for antimicrobial and supercapacitor applications. Surf Interfaces. 17, 100376. https://doi.org/10.1016/j.surfin.2019.100376

47. Krishnamoorthy K., Veerapandian M., Zhang L.H., Yun K., Kim S.J., 2012. Antibacterial efficiency of graphene nanosheets against pathogenic bacteria via lipid peroxidation. J Phys Chem C. 116, 17280–17287.https://doi.org/10.1021/jp3047054

48. Shubhangi M., Priyanka R., Ashish W., Sanjay M., 2014. Synthesis and comparative study of zinc oxide nanoparticles with and without capping of pectin and its application, World J Pharm Pharmaceut Sci. 3 (7), 1255–1267.

49. Jayaseelana C., Rahuman A. Abdul, Kirthi A. Vishnu, Marimuthu S., Santhoshkumara T., Bagavana A., Gauravb K., Karthikb L., Bhaskara Raob K.V., 2012. Novel microbial route to synthesize ZnO nanoparticles using *Aeromonas hydrophila* and their activity against pathogenic bacteria and fungi. Spectrochim. Acta A. 90, 78–84.

50. Halliwell B., Gutteridge J.M., 1989. Free radicals in biology and medicine, 2nd ed. Oxford: Clarendon Press.

51. Rehana D., Mahendiran D., Kumar R S., Rahiman A.K., 2017. In vitro antioxidant and antidiabetic activities of zinc oxide nanoparticles synthesized using different plant extracts. Bioprocess Biosyst Eng. 40, 943–957. https://doi.org/10.1007/s00449-017-1758-2

52. Muthuvel A., Jothibas M., Manoharan C., 2020. Effect of chemically synthesis compared to biosynthesized ZnO–NPs using Solanum nigrum leaf extract and their photocatalytic, antibacterial and invitro antioxidant activity. J Environ Chem Eng. 8, 103705. https://doi.org/10.1016/j.jece.2020.103705

53. Matussin S., Harunsani M.H., Tan A.L., Khan M.M., 2020. Plant-extractmediated SnO_2 nanoparticles: synthesis and applications. ACS Sustain Chem Eng. 8, 3040–3054.
https://doi.org/10.1021/acssuschemeng.9b06398

54. Zare M., Namratha K., Thakur M.S., Byrappa K., 2019. Biocompatibility assessment and photocatalytic activity of bio-hydrothermal synthesis of ZnO nanoparticles by Thymus vulgaris leaf extract. Mater Res Bull. 109, 49–59. https://doi.org/10.1016/j.mater resbull.2018.09.025

55. Bharathi D., Diviya Josebin M., Vasantharaj S., Bhuvaneshwari V., 2018. Biosynthesis of silver nanoparticles using stem bark extracts of Diospyros montana and their antioxidant and antibacterial activities. J Nanostruct Chem. 8, 83–92. https://doi.org/10.1007/s40097-018-0256-7

56. Das D., Nath B.C., Phukon P., Dolui S.K., 2013. Synthesis of ZnO nanoparticles and evaluation of

antioxidant and cytotoxic activity. Colloids Surf B Biointerfaces. 111, 556–560. https://doi. org/10.1016 /j.colsurfb.2013.06.041

57. Rahman A., Harunsani M.H., Tan A.L., Ahmad N., Khan M.M., 2021. Antioxidant and antibacterial studies of phytogenic fabricated ZnO using aqueous leaf extract of *Ziziphus mauritiana* Lam. Chemical Papers. 75(7), 3295-3308. https://doi.org/10.1007/s11696-021-01553-7

58. Xie Y., Yan B., Xu H., Chen J., Liu Q., Deng Y., Zeng H., 2014. Highly regenerable mussel-inspired Fe_3O_4@ polydopamine-Ag core–shell microspheres as catalyst and adsorbent for methylene blue removal. ACS Applied Materials & Interfaces. 6(11), 8845-8852. https://doi.org/10.1021/am501632f

59. Rad A.S., Mirabi A., Binaian E., Tayebi H., 2011. A review on glucose and hydrogen peroxide biosensor based on modified electrode included silver nanoparticles. Int J Electrochem Sci. 6(8) 3671-3683.

60. Murali M., Kalegowda N., Gowtham H.G., Ansari M.A., Alomary M.N., Alghamdi S., Shilpa N., Singh S.B., Thriveni M.C., Aiyaz M., Angaswamy N., 2021. Plant-mediated zinc oxide nanoparticles: Advances in the new millennium towards understanding their therapeutic role in biomedical applications. Pharmaceutics. 13(10), p.1662. https://doi.org/10.3390/pharmaceutics13101662

61. Siripireddy B., Mandal B.K., 2017. Facile green synthesis of zinc oxide nanoparticles by Eucalyptus globulus and their photocatalytic and antioxidant activity. Advanced Powder Technology. 28(3), pp.785-797. https://doi.org/10.1016/j.apt.2016.11.026